Self-Organized Unimolecular Polymers

Templating of Silsesquioxane Cross-Linking Using Unimolecular Self-Organizing Polymers**

Eric F. Connor, Linda K. Sundberg, Ho-Cheol Kim, Jeroen J. Cornelissen, Teddie Magbitang, Phil M. Rice, Victor Y. Lee, Craig J. Hawker, Willi Volksen, James L. Hedrick, and Robert D. Miller**

The assembly of structures, molecule by molecule, into a defined macroscopic or mesoscale object is known as the "bottom-up" approach to nanomanufacturing.[1] This approach will become more important in the semiconductor field, as dimensions continue to decrease. Modern chips contain up to 10 km of copper wiring, which can connect between 200 and 500 million silicon transistors on a single centimeter-sized chip. As a direct result of increasing wiring and device densities, insulating materials with lower dielectric constants will be required to mitigate signal delays and crosstalk while simultaneously decreasing electrical power consumption. For materials with dielectric constants $k < 2.0$, porosity is required, a factor fueling the current interest in porous films.[2]

While the incorporation of air ($k = 1.01$) significantly lowers the dielectric constant of any matrix polymer, to be useful for on-chip dielectrics, the pores in the foam must be 5–10 times smaller than the minimum device features, currently approaching 100 nm. Typically, nanoporosity is introduced into amorphous spin-applied films using sacrificial organic materials (porogens or pore generators).[3] With most macromolecular porogens, nanoscopic domains develop by a liquid–solid phase separation caused by cross-linking of the thermosetting resin; a typical nucleation and growth (NG) process.[4] To prevent macroscopic phase separation, the porogen must be initially miscible in the matrix. Subsequent curing of the resin results in both chemical changes and accompanying molecular-weight increases in the matrix, which drive the phase separation of the porogen. Ideally these nucleated polymer domains, which may consist of many polymer chains, remain nanoscopic in scale with growth inhibited by the cross-linking matrix (kinetically arrested growth), a process that is typically difficult to control.[3] In this communication, we describe the generation of a nanoporous material from an amorphous thermosetting prepolymer, where the porosity is generated from single polymer molecules that exhibit unimolecular self-organization. The process requires a stimuli-responsive, star-shaped copolymer that creates a nanosized domain[5] through a matrix-mediated collapse of the interior core of the core-corona polymeric structure (Figure 1 a–c). The outer corona of the star renders the insoluble core compatible with the thermosetting resin and suppresses aggregation or precipitation of the insoluble interior, so that a single polymer molecule templates cross-linking and ultimately generates a single hole. Other processes produce nanoporous thin films,[6] however, this simple approach does not require concurrent monomer hydrolysis to produce a prematrix or dynamic reorganization of amphiphilic polymers to produce supermolecular aggregates, but is a system that conforms with the rapid spin-and-bake sequence required for semiconductor manufacturing, while incorporating a control for nanoscopic pore size.

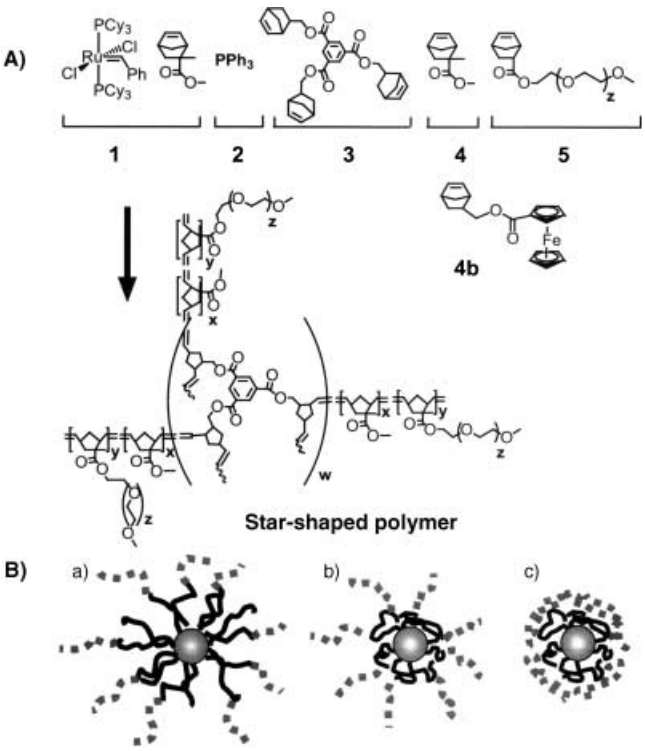

Figure 1. A) Outline of the stepwise synthesis of norbornene star-shaped copolymers (steps 1–5); B) solvent stimuli response of the unimolecular micelle: a) Swollen star polymer in good solvent for both the core and the corona; b) selective collapse of the hydrophobic core in a polar medium (e.g., MSSQ prepolymer); c) collapse of both the core and the corona in a poor solvent for both (e.g., cross-linked MSSQ).

A bottom-up route to unimolecular micellar star polymers using ruthenium-catalyzed ring-opening-metathesis polymerization (ROMP)[7] is described for the first time (details are provided in the Supporting Information). In a single pot,

[*] J. L. Hedrick, R. D. Miller, E. F. Connor, L. K. Sundberg, H.-C. Kim, J. J. Cornelissen, T. Magbitang, P. M. Rice, V. Y. Lee, C. J. Hawker, W. Volksen
IBM Almaden Research Center
650 Harry Road, San Jose, CA 95120 (USA)
Fax: (+1) 408-927-3310
E-mail: Hedrick@almaden.ibm.com
rdmiller@almaden.ibm.com

[**] Partial funding by the National Institute of Science and Technology (NIST) through an ATP cooperative agreement (70NANB8H4013) and the NSF Center for Polymeric Interfaces and Macromolecular Assemblies (CPIMA) is acknowledged. L.K.S. acknowledges partial financial support from JSR Microelectronics. The authors thank Eugene Delenia for expert assistance with TEM studies and Richard Siemens and Lucy Li for their definitive thermal analysis studies.

Supporting information for this article is available on the WWW under http://www.angewandte.org or from the author.

 DOI: 10.1002/ange.200350930

living oligomers (steps 1 and 2) are coupled to a polyfunctional cross-linking core (step 3) and the substructure is further elaborated by subsequent living polymerization (step 4), which generates additional arms (Figure 1). The reaction is completed by the addition of a norbornyl ester monomer containing a short polyethylene oxide (PEO) chain ($M_n = 2000$; step 5), to form the final "full star" that contains 30–40 wt % PEO incorporated in a comb architecture. The star polymers were subsequently hydrogenated for thermal and oxidative stability. By using a living polymerization technique, the molecular weight of the respective polymer chains can be controlled, a feature which ultimately governs both the size of the template and its relative hydrophilic/hydrophobic balance.

The size of the star polymer (as a solution in THF) was determined using dynamic light scattering (DLS).[8] In solution, a single star-shaped polymer assumes a solvent-swollen state and hence the values obtained by DLS represent the upper limit in size. The polymer samples (A and B, Table 1) were also studied by static light scattering (SLS), which provides both absolute molecular weights and the radius of gyration (R_g). The smaller star (polymer A) had an R_g value of 11.1 nm, while that of the larger star (polymer B) was 26.1 nm. The size distribution for both polymers was relatively narrow, consistent with the low-molecular-weight polydispersity index measured by both gel permeation chromatography (GPC) and SLS (Table 1). We used transmission electron microscopy (TEM) to estimate the sizes of the polymers in the dry state; under these conditions a single polymer molecule is assumed to be collapsed. To improve electron contrast for TEM imaging, star polymers analogous to samples A and B (GPC and DLS) that contained ferrocenyl monomer units were prepared. The ferrocenyl co-monomer (**4b**, Figure 1) was added after the core cross-linking step. From the TEM images of the star polymers, a number-average radius was calculated and taken as being representative of their templating size. The average radius for polymers A and B was 8.0 and 12.5 nm, respectively, with each sample showing a narrow size distribution (Figure 2). These particular micellar polymers are a convenient size for visualization by microscopy and to demonstrate the templating concept for the formation of amorphous porous materials.

The amphiphilic polymers (samples A and B) were dissolved in a solution containing methyl silsesquioxane (MSSQ) prepolymer in propylene glycol monomethyl ether and the resulting solution was spun on a silicon wafer to produce thin films. The sample was heated to 450 °C at a rate of 5 °C min^{-1}. During this process, the resin becomes progressively more cross-linked and hydrophobic as the initially present polar silanol end groups condense (150–250 °C). Upon further curing, the star polymer thermally degrades to low-molecular-weight products which vaporize (350–400 °C) to leave behind a hole or pore. For a true templated process,[9] the pore sizes should be independent of porogen concentration below the percolation threshold and reflect the actual size of the additive. This mechanism is distinguished from a NG process, where the domain sizes and shape depend strongly on porogen concentration, molecular weight, and processing conditions.[10a] Two cross-sectional TEM pictures illustrate the remarkable differences in the porous morphologies produced by NG and templating mechanisms (Figure 3). The NG morphology was generated using a linear methacrylate copolymer, which was initially miscible in the MSSQ resin.[10b] The pores generated through single-polymer templating (sample A) are clearly more regular in size and shape. Representative field-emission scanning electron microscopy (FE-SEM) of porous MSSQ produced from two different

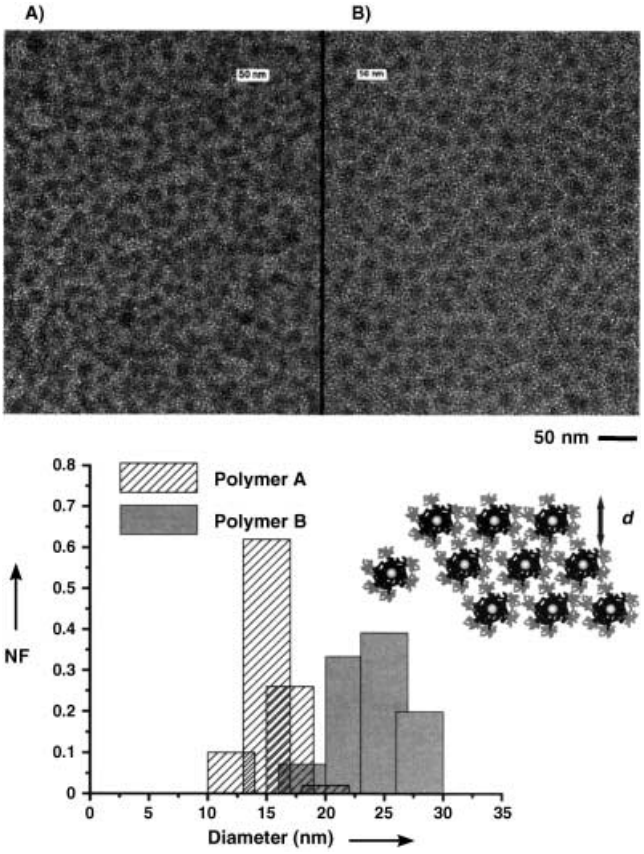

Figure 2. Above: TEM images of two different-sized star-shaped polynorbornene polymers (samples A and B, Table 1) containing ferrocene units (dark features) for contrast enhancement; below: size histograms produced from the TEM micrographs. NF = number fraction.

Table 1: Size characterization of the amphiphilic star polymer by dynamic light scattering, static light scattering, and TEM analysis.

Polymer sample	QR_n [nm]	R_g [nm]	R_{hs} [nm]	M_w [$\times 10^{-6}$ g mol^{-1}]	QR_w/R_n	SR_w/R_n	PD	TEM R_n [nm]
A	10.8	11.1	14.3	0.35	1.09	1.06	1.15	8.0
B	23.8	26.1	33.6	1.82	1.21	1.30	1.30	12.5

QR_n = hydrodynamic radius (DLS in tetrahydrofuran). R_g = radius of gyration (SLS in tetrahydrofuran). R_{hs} = hard sphere radius [$(5/3)^{0.5} \times R_g$]. QR_w/R_n = polydispersity determined by DLS. SR_w/R_n = polydispersity determined by SLS. M_w = molecular weight determined by SLS. PD = polydispersity determined by GPC. TEM R_n = number average radius, derived from transmission electron microscopy.

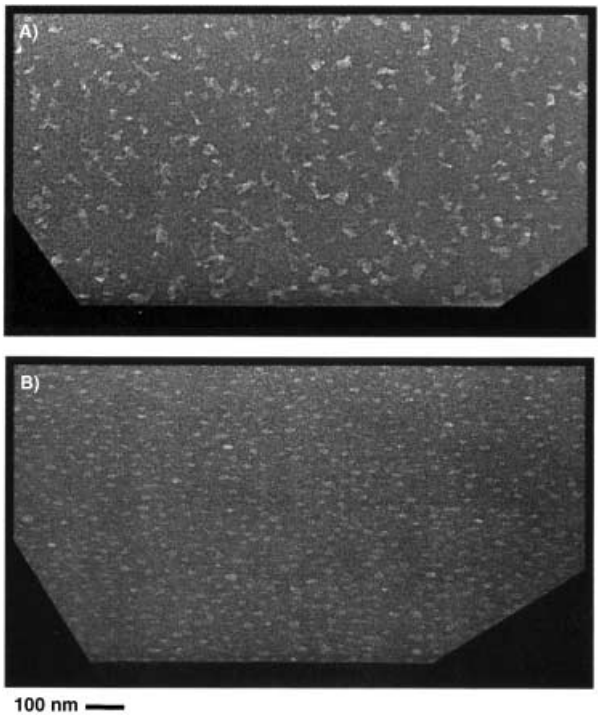

Figure 3. TEM pictures showing the differences in porous morphologies generated by: A) Nucleation and growth (NG),[9] and B) unimolecular templating techniques.

micellar poly(norbornene) loading levels (10 and 30 wt%) are shown in Figure 4 (the upper concentration limit for this star polymer/silsesquioxane system is around 35 wt%, above which aggregation begins to occur). The pore sizes in each sample are similar and a compositional invariance of morphology is observed; that is, only the pore density increases with loading level. For a templating process, two star polymers differing in size (for example, samples A and B, Table 1) should produce foams with hole sizes reflecting the respective porogen dimensions. Two cross-sectional TEM micrographs of these respective films are shown (Figure 5). Curiously, the pores are slightly elliptical, that is, elongated in the wafer plane, a feature that could result from a number of conditions; for example, the radial shear stresses produced during spinning, partial in-plane pore collapse, or perhaps as a result of the focussed ion beam (FIB) procedure used to prepare the sample (this effect is under investigation). The histograms generated for the porous films show that the hole sizes (measured along the longest axis) in the matrix resin (Figure 5) correlate with the dry size of the micellar polymers measured by TEM (Figure 4). Also, the distribution in pore size reflects the size dispersity of the polymer samples. These data collectively provide strong evidence that the star polymers behave as a unimolecular template during MSSQ vitrification. This particle-like behavior occurs in spite of the fact that cross-linking in the porogen is minimal and confined to a small molecular core.

Thermal analysis by dynamic mechanical analysis (DMA) of the micellar star polymers in the hybrid samples (see Supporting Information) confirms that at least the internal hydrophobic core of the micellar polymers is phase-separated

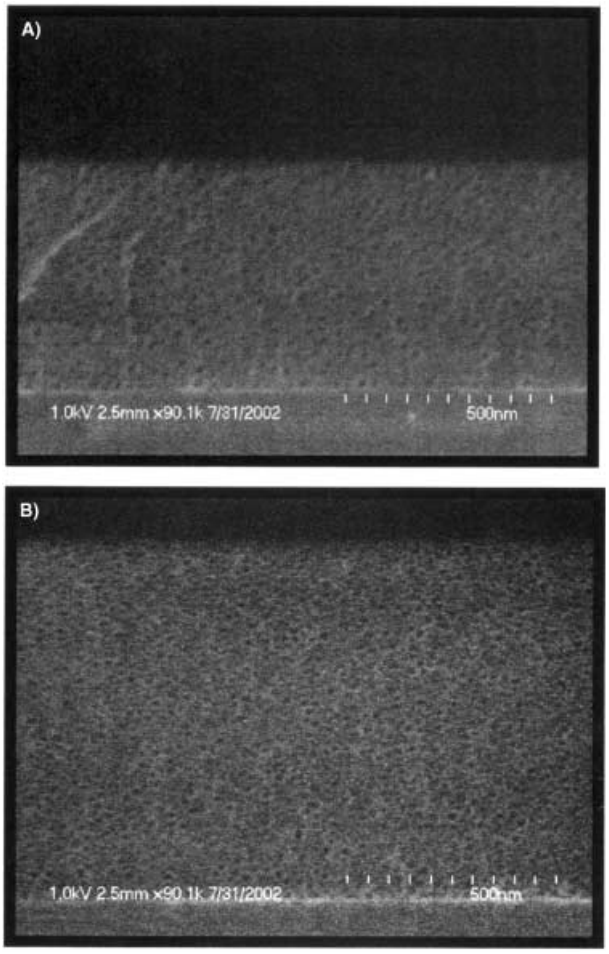

Figure 4. FE-SEM images of nanoporous MSSQ generated using different loadings of a unimolecular self-assembling star-shaped polymer (sample A, Table 1): A) 10 wt%; B) 30 wt%.

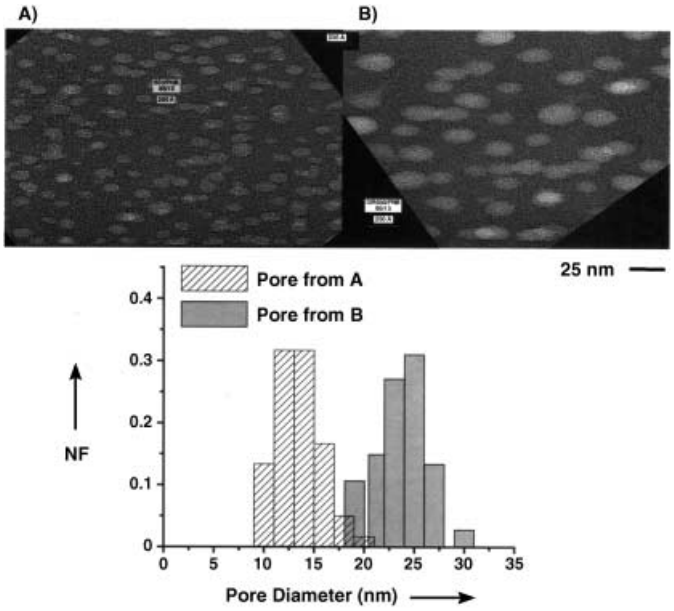

Figure 5. Above: TEM pictures of two porous MSSQ samples prepared from two different-sized star polymers (samples A and B, Table 1); below: size histograms produced from the TEM micrographs. NF = number fraction.

from the MSSQ resin after soft curing (150 °C). The PEO arms are ultimately expelled during further curing (to 200 °C) by frustrated phase separation generating the single-polymer templating morphology.[11] The dielectric constants of the porous samples (see Supporting Information) decrease predictably from 2.8 to 1.7 with increasing porogen loading (0–50 %).

In summary, unimolecular amphiphilic star polymers, synthesized by ROMP procedures, provide a controlled templating effect during the thermal cure of amorphous silsesquioxane derivatives. The unimolecular nature of the polymeric micellar materials eliminates the complex dynamic assembly characterizing most amphiphilic systems. Porogen burnout results in nanoporous films where the pore sizes and distributions reflect the dimensions of single polymer molecules. By using controlled chemical synthesis to produce defined macromolecules, macroscopic nanostructured thin films of technological utility are produced providing a cogent example of the evolution from nanoscience to nanotechnology. Additional applications of unimolecular micellar templating will be discussed in future publications.

Received: January 13, 2003 [Z50930]
Published online: July 28, 2003

Keywords: metathesis · nanoporous materials · polymers · self-assembly · template synthesis

[1] H. Doumanidis, *Nanotechnology* **2002**, *13*, 248.
[2] R. D. Miller, *Science* **1999**, *286*, 421.
[3] a) J. L. Hedrick, T. Magbitang, E. F. Connor, T. Glauser, W. Volksen, C. J. Hawker, V. Y. Lee, R. D. Miller, *Chem. Eur. J.* **2002**, *8*, 3308; b) S. Yang, P. A. Mirau, C. S. Pai, O. Nalamasu, E. Reichmanis, J. C. Pai, Y. S. Obeng, J. Seputro, E. K. Lin, H. J. Lee, J. N. Sun, D. W. Gidley, *Chem. Mater.* **2002**, *14*, 369.
[4] J. Kiefer, J. L. Hedrick, J. G. Hilborn, *Adv. Polym. Sci.* **1999**, *147*, 161.
[5] a) M. Antonietti, R. Basten, S. Lohmann, *Macromol. Chem. Phys.* **1995**, *196*, 441; b) K. L. Wooley, *J. Polym. Sci. Part A* **2000**, *38*, 1397.
[6] S. Polarz, M. Antonietti, *Chem. Commun.* **2002**, *22*, 2593.
[7] a) T. M. Trnka, R. H. Grubbs, *Acc. Chem. Res.* **2001**, *34*, 18; b) C. W. Bielawski, R. H. Grubbs, *Macromolecules* **2001**, *34*, 8838.
[8] C. Graf, W. Schartl, K. Fischer, N. Hugenberg, M. Schmidt, *Langmuir* **1999**, *15*, 6170.
[9] D. Y. Zhao, J. L. Feng, Q. S. Huo, N. Melosh, G. H. Fredrickson, B. F. Chmelka, G. D. Stucky, *Science* **1998**, *279*, 548.
[10] a) E. Huang, M. F. Toney, W. Volkesen, D. Mecerreyes, P. Brock, H. C. Kim, C. J. Hawker, J. L. Hedrick, V. Y. Lee, T. Magbitang, R. D. Miller, *Appl. Phys. Lett.* **2002**, *81*, 2232; b) Q. R. Huang, W. Volksen, E. Huang, M. Toney, C. W. Frank, R. D. Miller, *Chem. Mater.* **2002**, *14*, 3676.
[11] E. A. Turi, *Thermal Characterization of Polymeric Materials, Vol. 1*, Elsevier/Academic Press, London, **1997**.

